Characteristics of the Elevation Drive Suspension of the 64-Meter Antennas

H. D. McGinness
Ground Antennas and Facilities Engineering Section

The elevation axis drive unit of the DSN 64-m antennas is arranged so that its output pinion can self-align to the bull gear. The design is described and conflicting desiderata are discussed.

I. Introduction

The elevation drives for the 64-m antennas at DSS 14, 43, and 63 have been in operation for 18, 12, and 11 years respectively. During these periods only a moderate amount of maintenance has been required. There has gradually developed, however, an unusual wear pattern on both the pinions and bull gears. It is the intent of this report to review some of the design features of the elevation drive suspension and to discuss why certain changes were made and whether these changes are related to the gear wear.

II. Description of the Drive System

A pair of bull gear segments of 12.65-m radii are concentric with the elevation axis and spaced approximately 5.4 m apart. The output pinions of two drive units mesh with each bull gear and are counter-torqued against each other so that backlash in the gear system is eliminated. Reference 2 contains a good general description of the drive system. Figures 1 and 2 show schematic views of the upper and lower drive units and their relationship to the bull gear. From these figures it may be seen that the output pinions are self-aligning to the bull gear. Such a large bull gear is likely to have radial and lateral runouts as well as twist. A fixed drive pinion would be subjected to misalignment and perhaps excessive change in gear contact ratio. A perfect self-aligning arrangement would obviate these undesirable features.

From Fig. 1 it may be seen that the lower end of the drive unit is ball-joint mounted to the antenna alidade and that this ball joint lies on a tangent line to the bull gear-pinion pitch line. The reaction roller is directly opposite the output pinion and rolls on the inside surface of the bull gear ring so as to keep the pinion properly spaced with respect to the bull gear teeth. The load on the reaction roller ideally is equal to the separating force between the pinion and bull gear. The dead weight of the drive unit, or gear box, is carried ideally by the alidade ball joint and by the two vertical spring-loaded struts labeled F_1 and F_2 in the figures. Horizontal stability is provided by the horizontal spring-loaded strut labeled S. With respect to the alidade ball joint and the tangent line, the gear box can pitch, yaw, and roll, as the bull gear runs out radially,

laterally, and in a twisting fashion. As these aberrant displacements occur, the reaction roller force and the strut forces change.

III. Characteristics of These Self-Aligning Gear Boxes

The gear box is installed by hoisting it to a position near its final position, attaching the ball-joint pivot to the alidade, placing auxiliary jacks appropriately to support the remaining weight, and installing the horizontal and vertical spring loaded struts which have been set to a calculated length by displacement of the springs by auxiliary bolts. Then the auxiliary jacks are removed, thus allowing the weight to be transferred to the reaction roller and the vertical struts. The auxiliary bolts holding the springs are removed and the strut lengths adjusted until the load is removed from the reaction roller. To limit the amount of strut length adjustment to a practical value requires that the vertical strut spring constants not be too low. On the other hand it is desirable to have low spring constants in the vertical struts so that when the bull gear runs out radially, there will not be an excessive transfer of load to the reaction roller. Additionally, it is desirable that the ratio of the stiffness of the vertical struts be a particular value such as to allow gear box pitch unaccompanied by gear box roll. For example, if the bull gear runs out radially but does not twist, the vertical struts should extend (or compress) by amounts which do not induce gear box roll, since unwanted roll represents a misalignment. The correct extension ratio is a function of the strut configuration, and extension ratio is proportional to the strut stiffness ratio.

There are schematic drawings of the three struts in Fig. 3. The horizontal strut, S, is preloaded to 1156 N and has a spring constant of 38876 N/m in either tension or compression. In order to allow gear box yaw to accommodate tooth misalignment, the horizontal strut stiffness should be low. On the other hand, it must be high enough to insure stability against the gear box running off the bull gear when the bull-gear motion is directed from pinion to alidade ball joint. The Number 1 gear box ran off the bull gear twice in 1966. Most of the time this gear box was stable and none of the other three ever ran off. A probable explanation of why this gear box ran off the bull gear is given in the analysis of Appendix A, the result of which defines a critical lateral displacement (see Figs. 30 and 31).

The derivation of the proper ratio between the vertical strut extensions, and the related stiffness ratio, is given in the analysis of Appendix B (see Figs. 4 and 5).

An outline of the method of installing the struts and aligning the gear boxes is given in Appendix C.

IV. Results of the Analyses

The analysis of Appendix A suggested that the value of the critical lateral displacement, x_{CR} for gear box No. 1 was abnormally small because there was an excessive amount of dead weight loading on the reaction roller. The analysis of Appendix B showed that the stiffness ratio between the original vertical struts was not very close to the ideal value. In order to reduce the dead weight loading on the reaction roller, it would have been necessary to change the strut lengths slightly. Although length adjustments were built into the original struts, it was found that the adjusting nut on the large vertical compressive strut could not be turned. A study was conducted to decide whether new and properly designed spring loaded struts or servo controlled constant force hydraulic struts should be employed. It was decided that properly designed spring loaded struts would be more reliable and less expensive. Such struts were fabricated and tested for stiffness at the fabricator's plant. The new compression strut is shown schematically in Fig. 3(c). It incorporates a ball bearing on the upper end of the bronze adjusting nut. Length adjustment of 4.233 mm per turn can be made with moderate torque. The new tension strut shown in Fig. 3(b) also employs a bronze adjusting turnbuckle nut one turn of which changes the strut length by 4.233 mm. These were installed at DSS 14 in July of 1982 and at DSS 43 and DSS 63 later in the same year.

The load-deflection curves of all the new compression and tension struts are shown in Figs. 6 through 29. The Belleville spring elements used in the vertical struts were selected from catalogs. An advantage of Belleville disks is that the stiffness of the assembly can be altered by adding or subtracting disks. The test performance of the tension struts was generally very good and corresponded fairly well with calculations made in accordance with Ref. 3. The first tests on the compression struts, which contained much larger disks, were very erratic and unrepeatable. Many of these elements had to be sent back to the manufacturer for rework which consisted of grinding true flats near the outer and inner edges. Without these small edge flats there was the tendency for one or more elements to move laterally and wedge against the housing, thereby producing unrepeatable results. The final performance of the compression struts was very good as is indicated in Figs. 6 through 17. Because of the tendency of some of the spring elements to wedge against the housing, it is recommended that if a strut unit must be disassembled, that each spring element be marked for angular orientation and position in the stack, and upon reassembly this sequence and angular orientation be reestablished.

Table 2 of Appendix B lists the stiffness ratios of all the vertical strut pairs, K_1/K_2. From this table it may be seen that all the ratios are within the ranges judged to be satisfactory

from the standpoint of preventing unwanted roll when the gear box must move to accommodate bull gear radial runout.

The gear box weights, center of gravity position, and the strut locations given in Figs. 1 and 2 are believed to be accurate because they were determined by measurement. In December 1981 one upper and one lower gear box were suspended by a cable harness so that the tangent line angles of 42.25° and 7.683° of Figs. 1 and 2 were obtained. The harness was attached to a load cell which determined the total weight. The center of gravity lay directly beneath the single cable supporting the load cell. The strut locations were verified by surveying methods.

An outline of how the new struts were installed and how the reaction roller was aligned is given in Appendix C. After the new struts were so installed and aligned the antenna was driven back and forth many times through the 85° elevation range and lateral runout of the pinion with respect to the bull gear was observed to be less than 4 mm.

V. Conclusion

The new elevation drive vertical struts allow the roll alignment of the drive pinion and reaction roller to be made perfect at any particular elevation angle. The stiffness ratio of the two vertical struts is such that the roll alignment should remain perfect even though the bull gear has radial runout. The ease of adjusting the strut lengths allows the reaction roller to be set so that it carries no dead weight load at the elevation angle at which it was adjusted. Moderate amounts of bull gear radial runout or twist will not cause the reaction roller to be overloaded.

The original vertical struts were very difficult to adjust and best alignment was not maintained. This probably caused some excessive wear of the gear teeth near their edges; however, it is believed that such misalignment is not the primary cause of the strange wear pattern which exists over the entire width of the gear teeth and that other reasons should be sought.

References

1. McGinness, H., 1982, Lateral and drag forces on misaligned cylindrical rollers, *TDA Progress Report 42-69*, 174-178, Jet Propulsion Laboratory, Pasadena, Calif.
2. The NASA/JPL 64-m Diameter Antenna at Goldstone, CA: Project Report TM 33671, 19XX, pp. 66-108 (internal document).
3. Almen, I. O., and A. Laszlo, 1936, The Uniform Section Disc Spring, *ASME Trans. 58*, 305-314.

Table 1. Ideal ratio between strut stiffness

	$\lambda = \frac{K_1}{K_2}$	$\frac{h}{\varrho_R}$
Lower	0.694	0.01554
	0.460	-0.01535
Upper	0.760	0.01533
	0.446	-0.01558

Table 2. Stiffness ratios of vertical struts

Elevation Gear Drive No.	Tension Strut Serial No.	Comp. Strut Serial No.	K_1 Comp., lb/in.	K_2 Tension, lb/in.	$\frac{K_1}{K_2}$
DSS-14 I *L*	2	5	3055	5438	$0.46 < 0.562 < 0.694$
DSS-14 II *U*	1	1	2829	5510	$0.44 < 0.513 < 0.760$
DSS-14 III *L*	4	3	2837	5142	$0.46 < 0.552 < 0.694$
DSS-14 IV *U*	3	2	2878	5117	$0.44 < 0.562 < 0.760$
DSS-43 I *L*	11	12	3243	5172	$0.46 < 0.626 < 0.694$
DSS-43 II *U*	12	11	3144	5177	$0.44 < 0.607 < 0.760$
DSS-43 III *L*	10	4	3125	5056	$0.46 < 0.618 < 0.694$
DSS-43 IV *U*	9	10	3504	5312	$0.44 < 0.660 < 0.760$
DSS-63 I *L*	8	6	3472	5113	$0.46 < 0.679 < 0.694$
DSS-63 II *U*	7	8	3315	5172	$0.44 < 0.641 < 0.760$
DSS-63 III *L*	6	7	3760	5420	$0.46 < 0.693 < 0.694$
DSS-63 IV *U*	5	9	3488	5357	$0.44 < 0.651 < 0.760$

Table 3. Vertical strut alignment dimensions at DSS-14

Elevation Angle at Which Struts Were Adjusted, deg	Elevation Drive Gear Box No.	Comp. Strut Serial No.	Dimension *A*, mm	Dimension *B*, mm	Ten. Strut Serial No.	Dimension *a*, mm	Dimension *b*, mm
65	I	5	53.6	139.7	2	68.1	60.5
60	II	1	63.0	152.4	1	71.9	57.2
71	III	3	59.4	106.4	4	66.8	63.5
71	IV	2	63.5	136.7	3	64.8	73.2

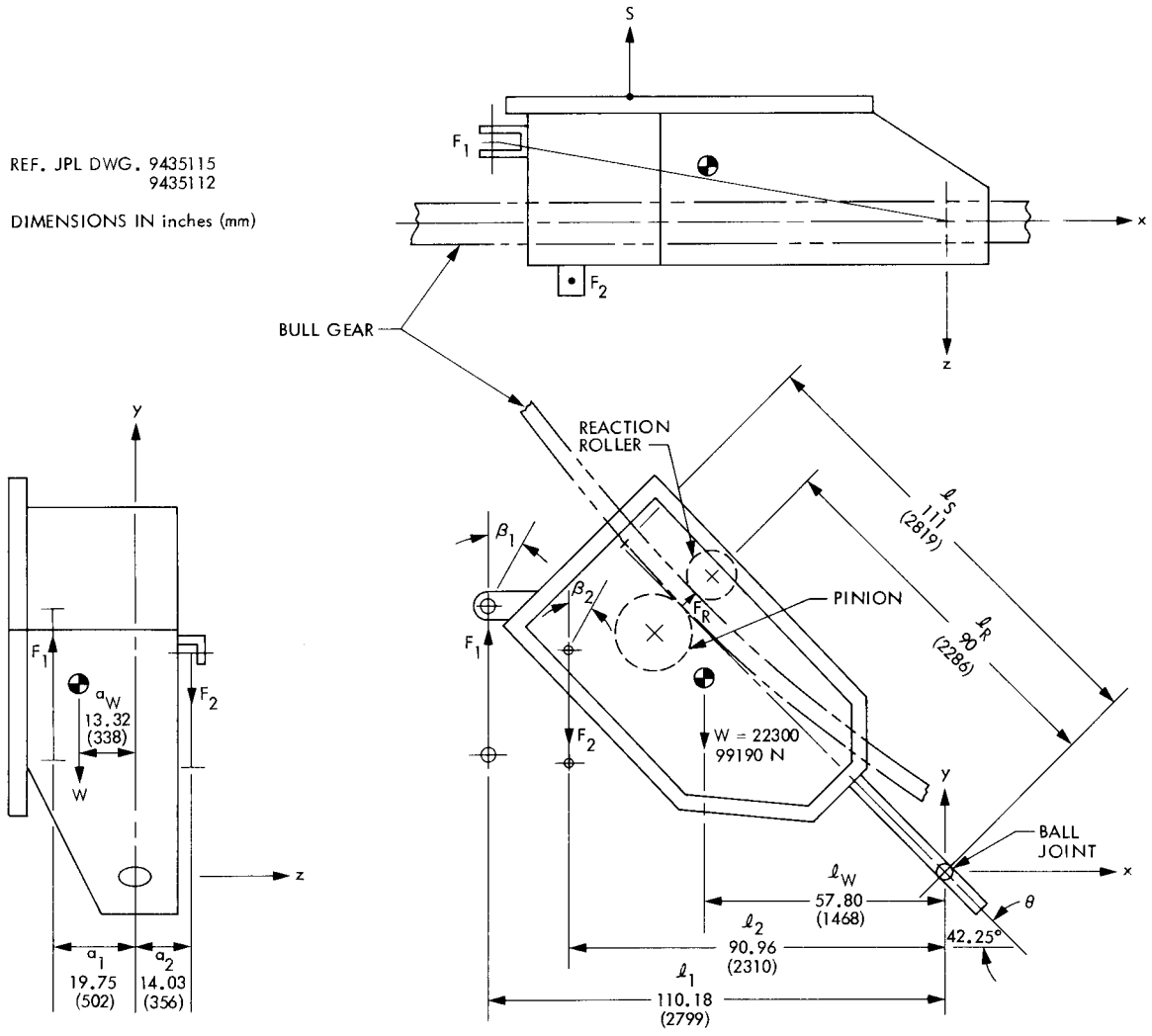

Fig. 1. Upper elevation drive gear box no. 2

REF. JPL DWG. 9435115
9435110

DIMENSIONS IN inches (mm)

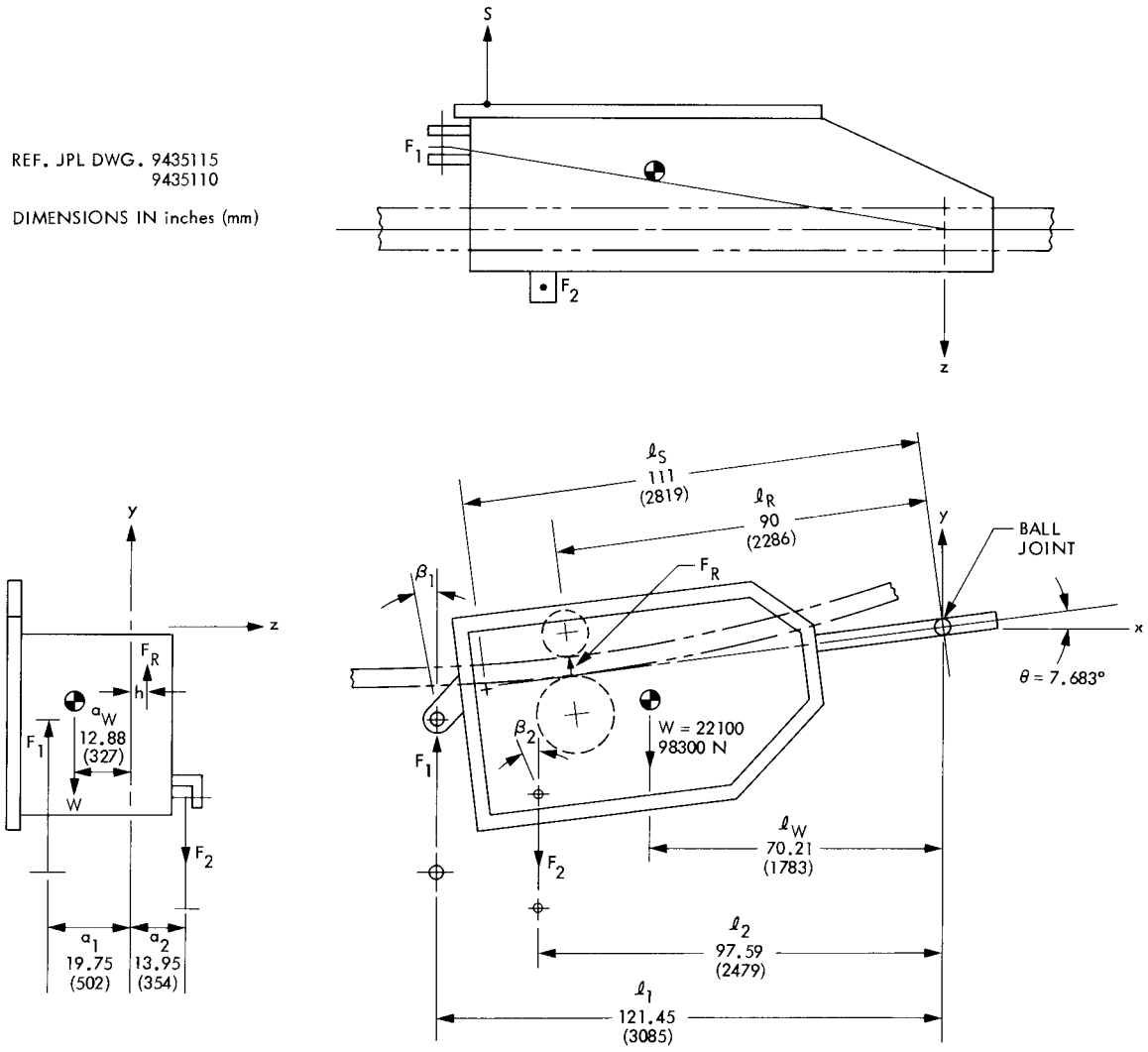

Fig. 2. Lower elevation drive gear box no. 3

(a) HORIZONTAL STRUT S TENSION OR COMPRESSION
(SEE JPL 9436181)

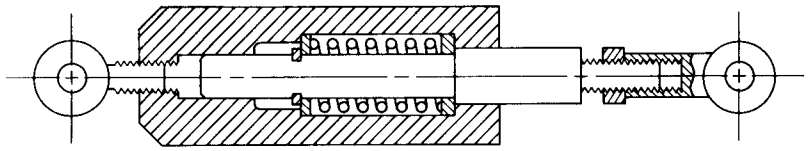

(b) VERTICAL STRUT F_2 TENSION ONLY
(SEE JPL 9477064)

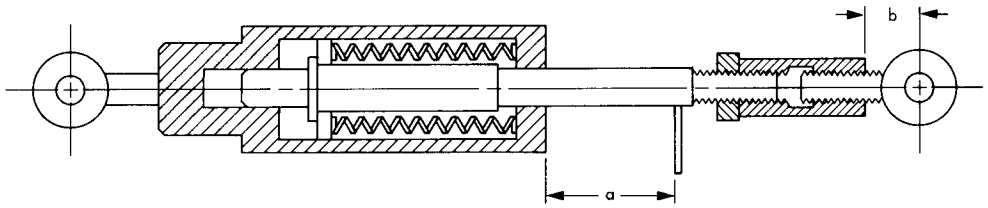

(c) VERTICAL STRUT F_1 COMPRESSION ONLY
(SEE JPL 9477064)

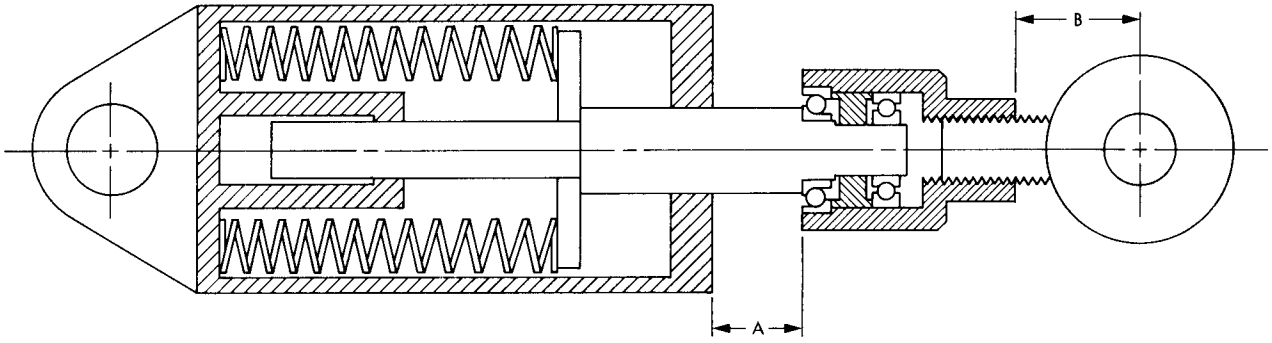

Fig. 3. Schematic drawings of elevation drive spring loaded support struts

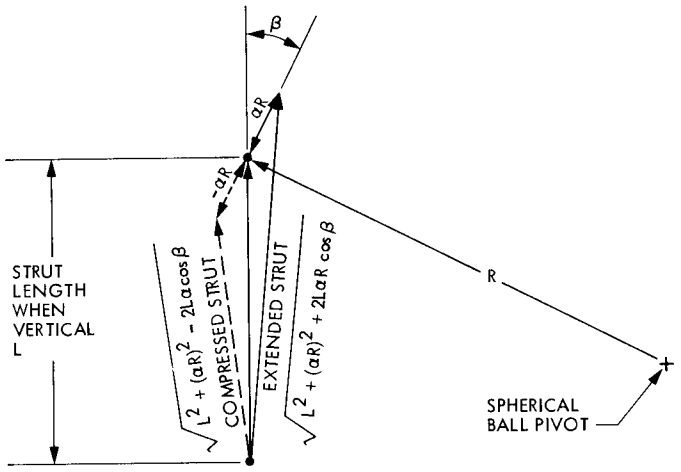

Fig. 4. Vertical strut length geometry

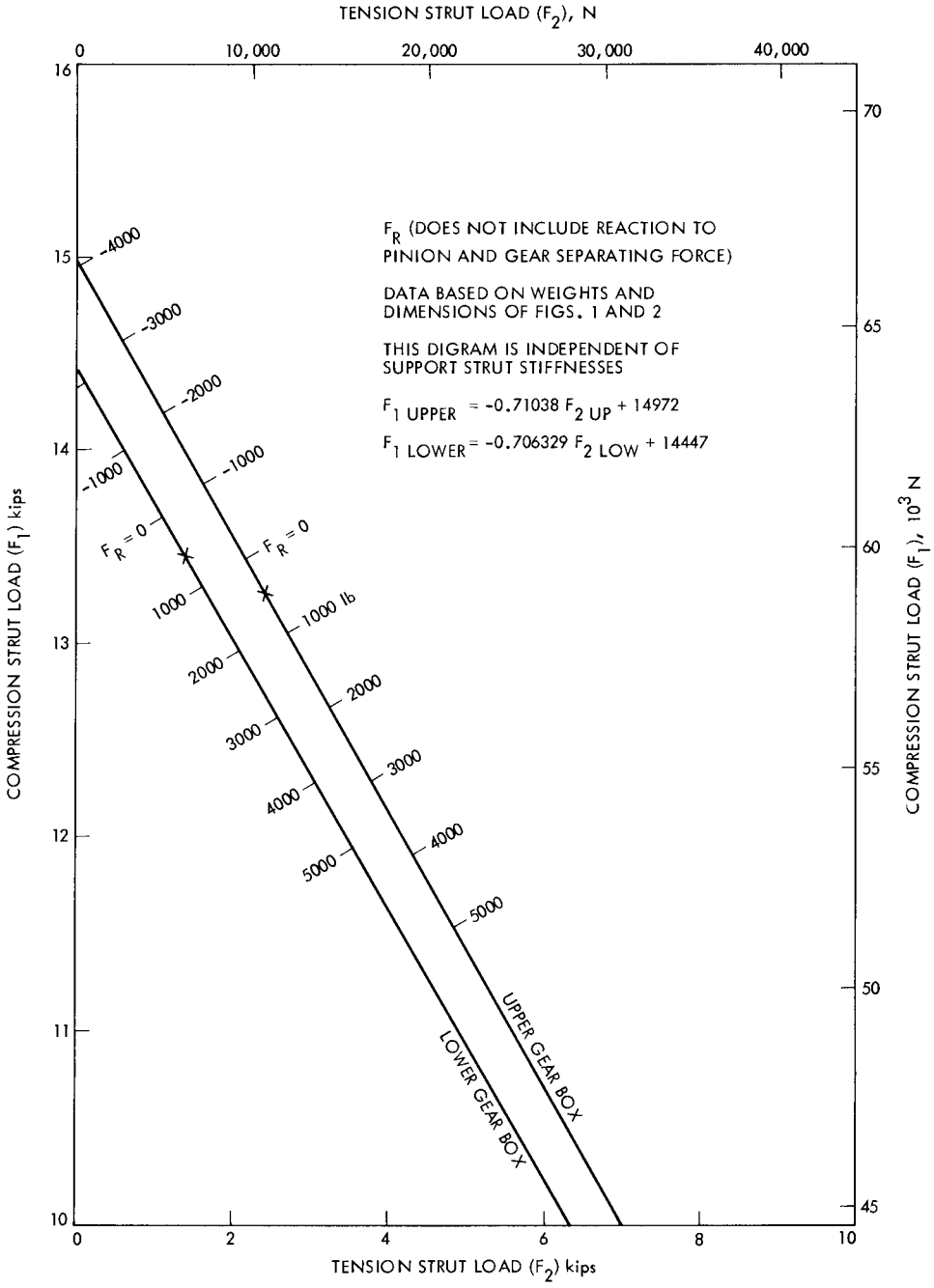

Fig. 5. F_1 versus F_2 for various values of roller reaction force F_R centered at mid-point of roller

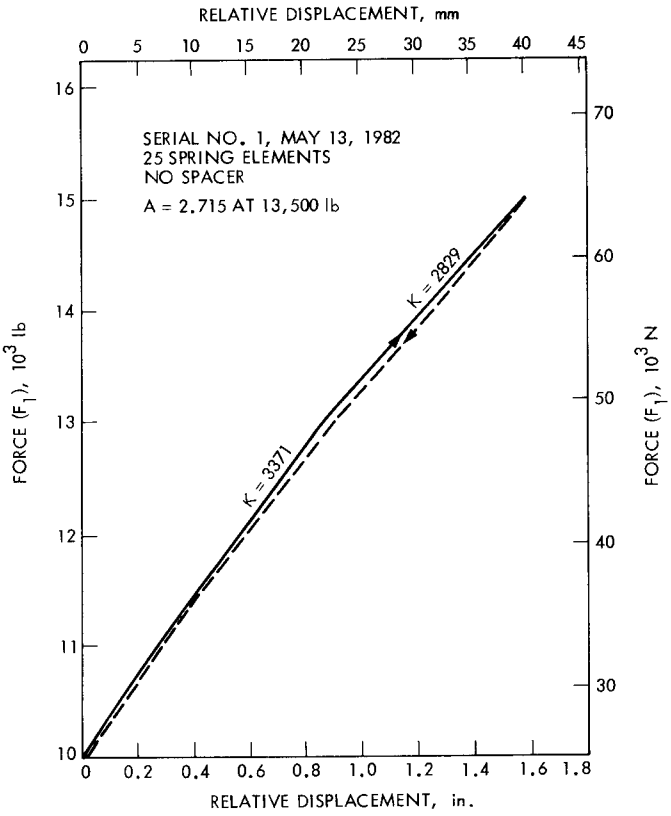

Fig. 6. Force versus deflection, measured, compression serial 1

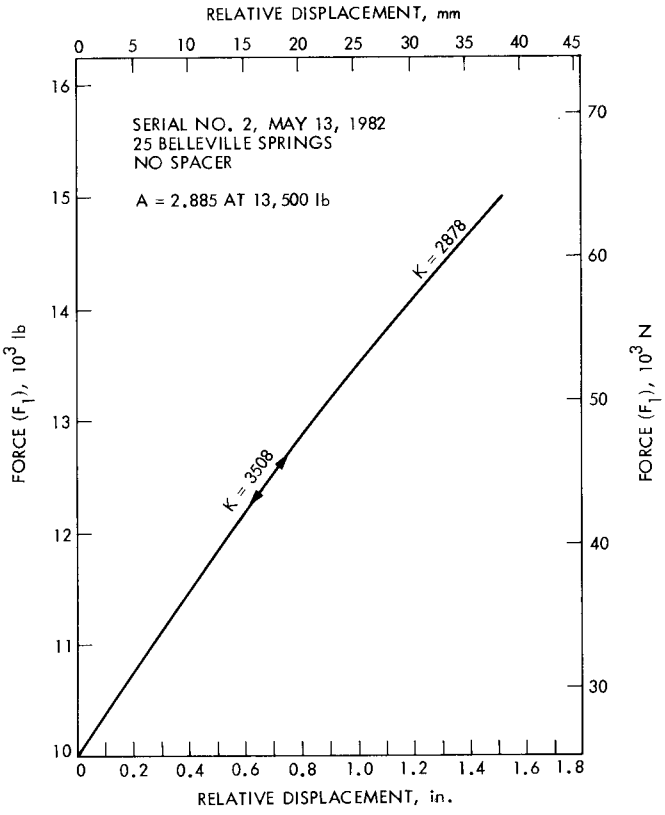

Fig. 7. Force versus deflection, measured, compression serial 2

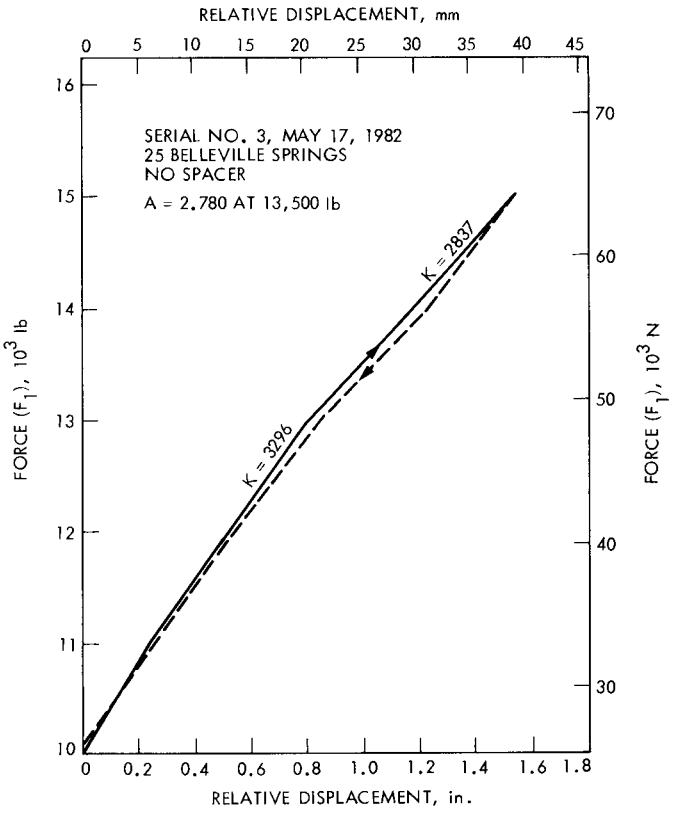

Fig. 8. Force versus deflection, measured, compression serial 3

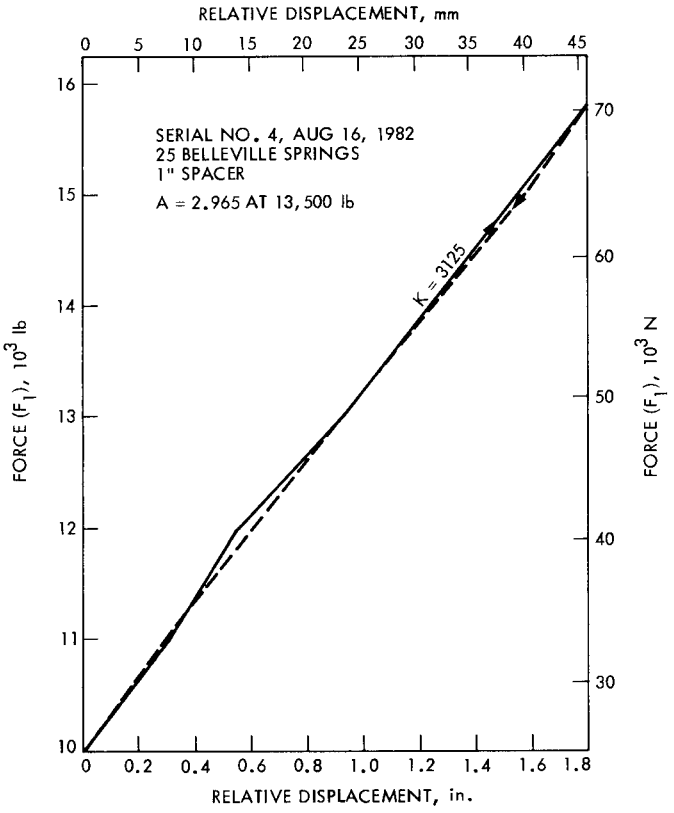

Fig. 9. Force versus deflection, measured, compression serial 4

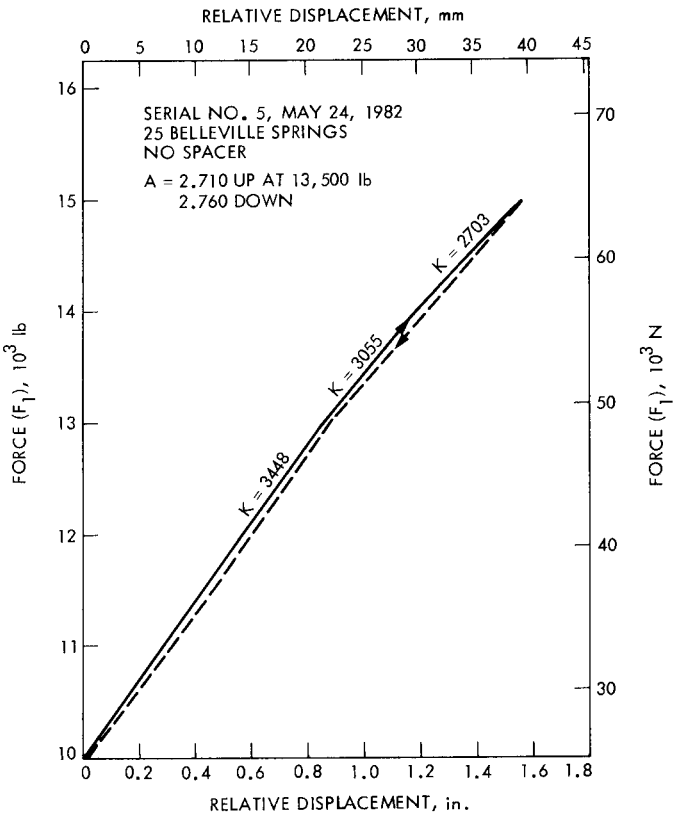

Fig. 10. Force versus deflection, measured, compression serial 5

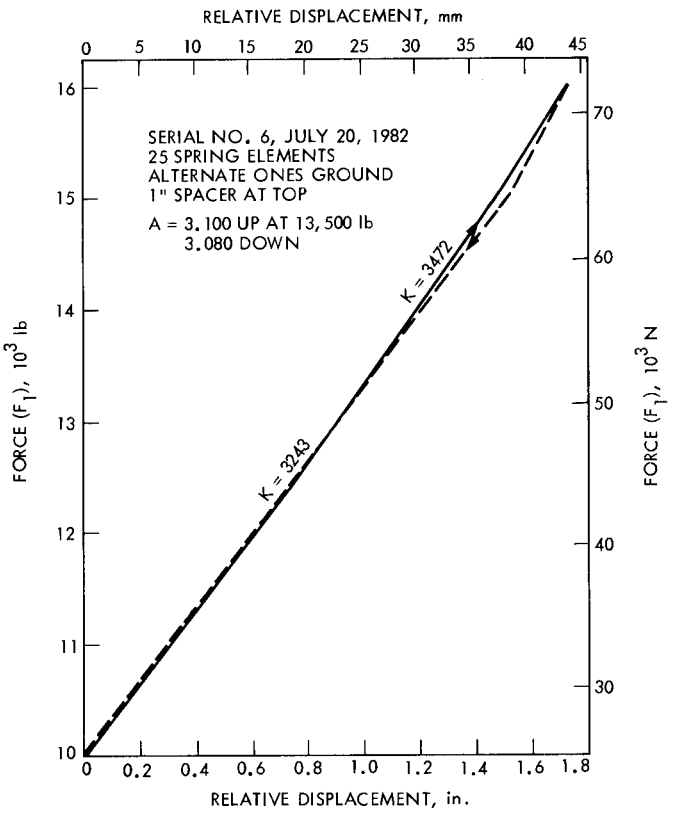

Fig. 11. Force versus deflection, measured, compression serial 6

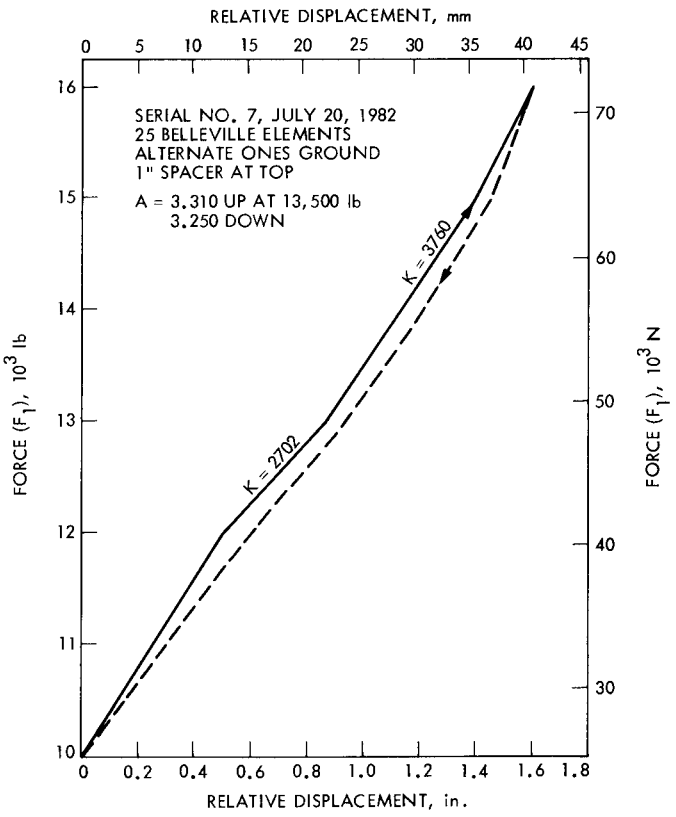

Fig. 12. Force versus deflection, measured, compression serial 7

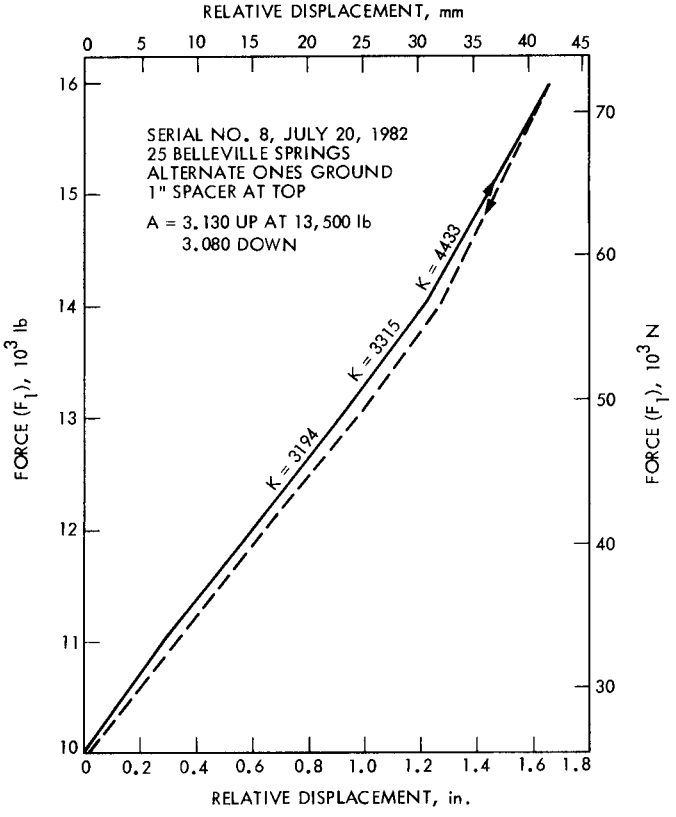

Fig. 13. Force versus deflection, measured, compression serial 8

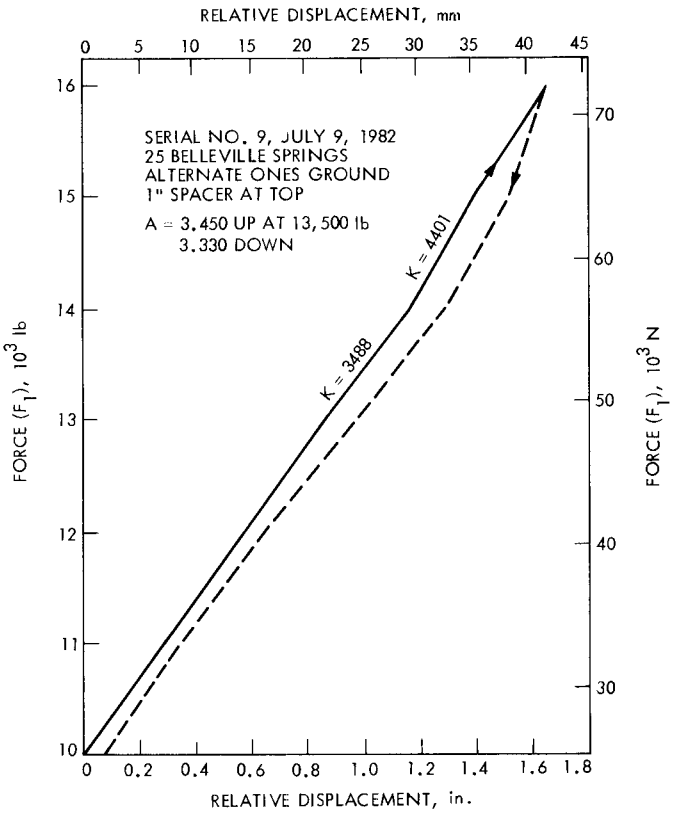

Fig. 14. Force versus deflection, measured, compression serial 9

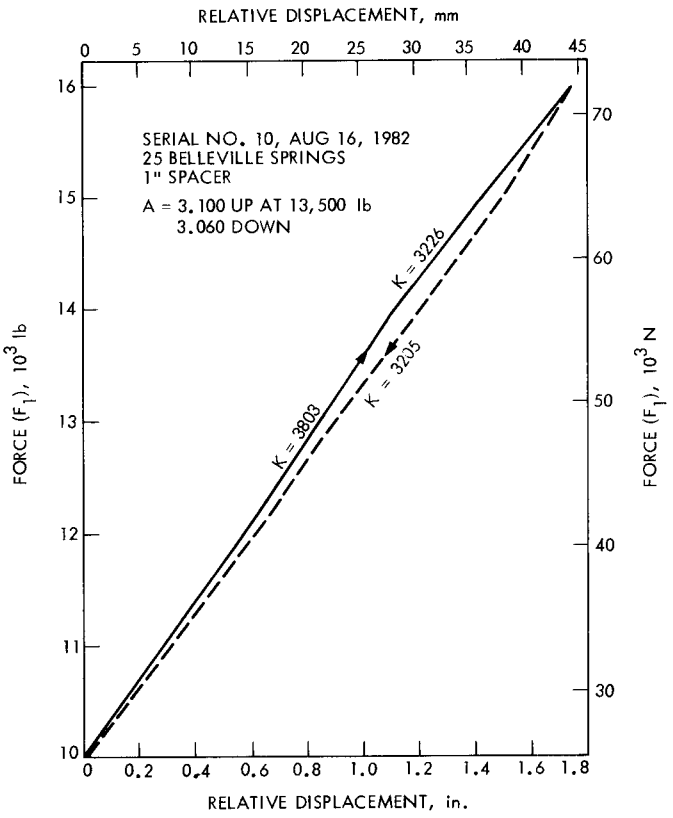

Fig. 15. Force versus deflection, measured, compression serial 10

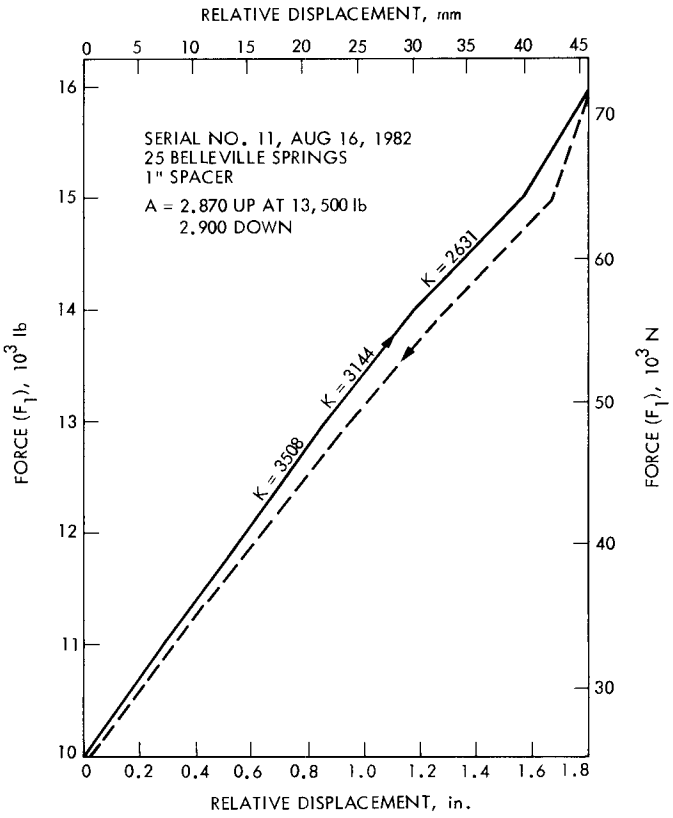

Fig. 16. Force versus deflection, measured, compression serial 11

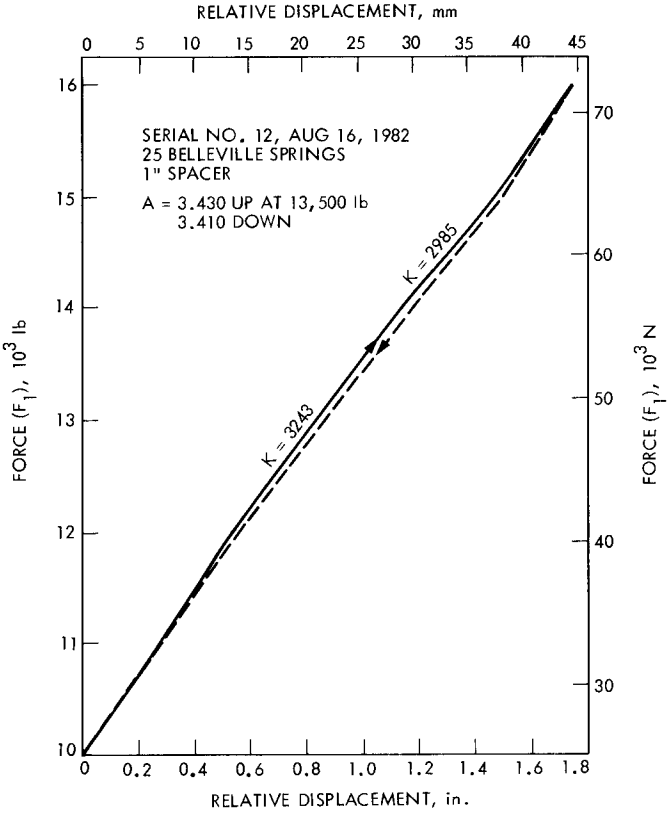

Fig. 17. Force versus deflection, measured, compression serial 12

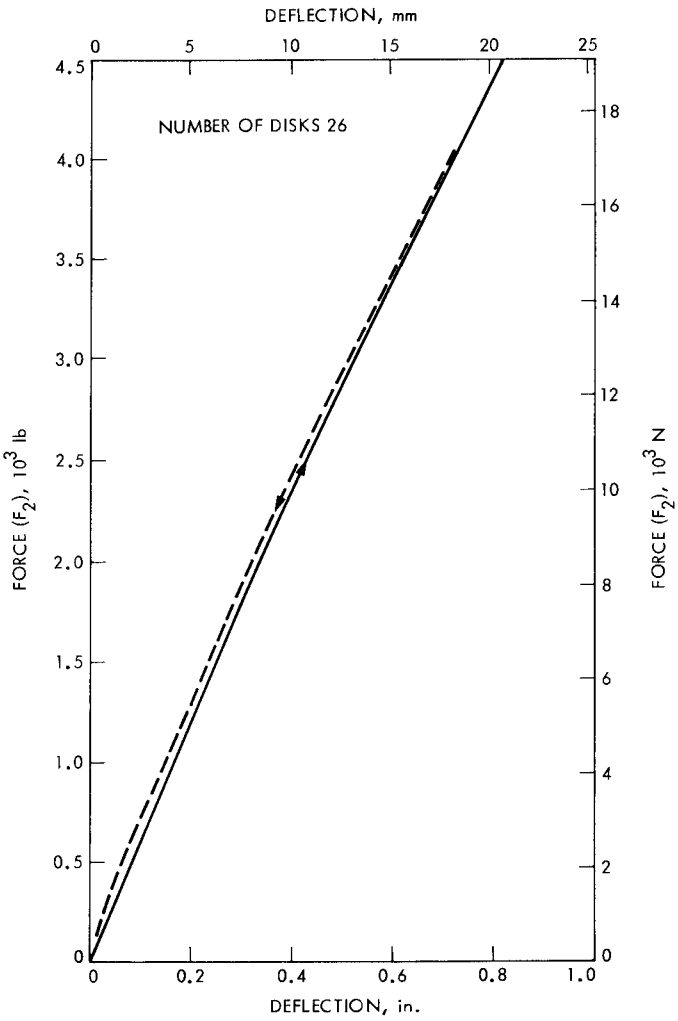

Fig. 18. Force versus deflection, measured, tension serial 1

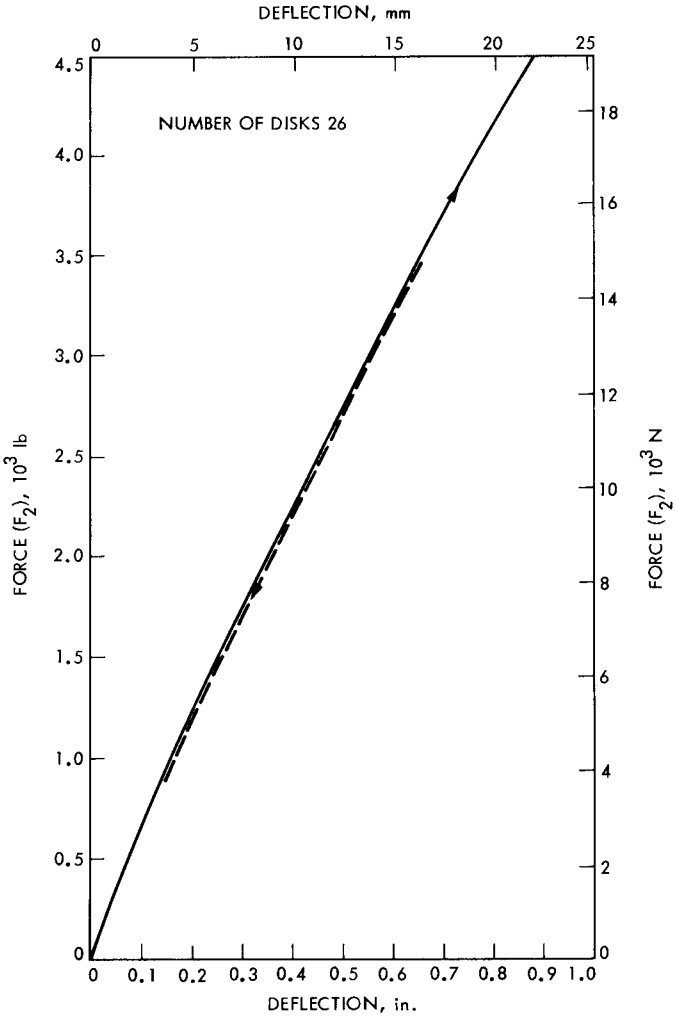

Fig. 19. Force versus deflection, measured, tension serial 2

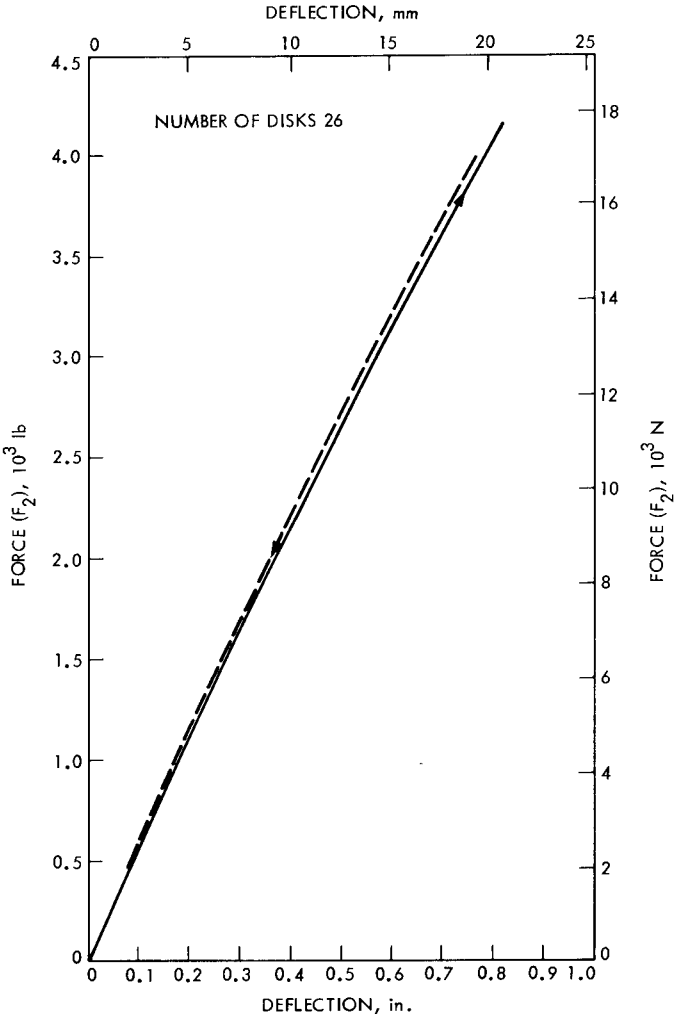

Fig. 20. Force versus deflection, measured, tension serial 3

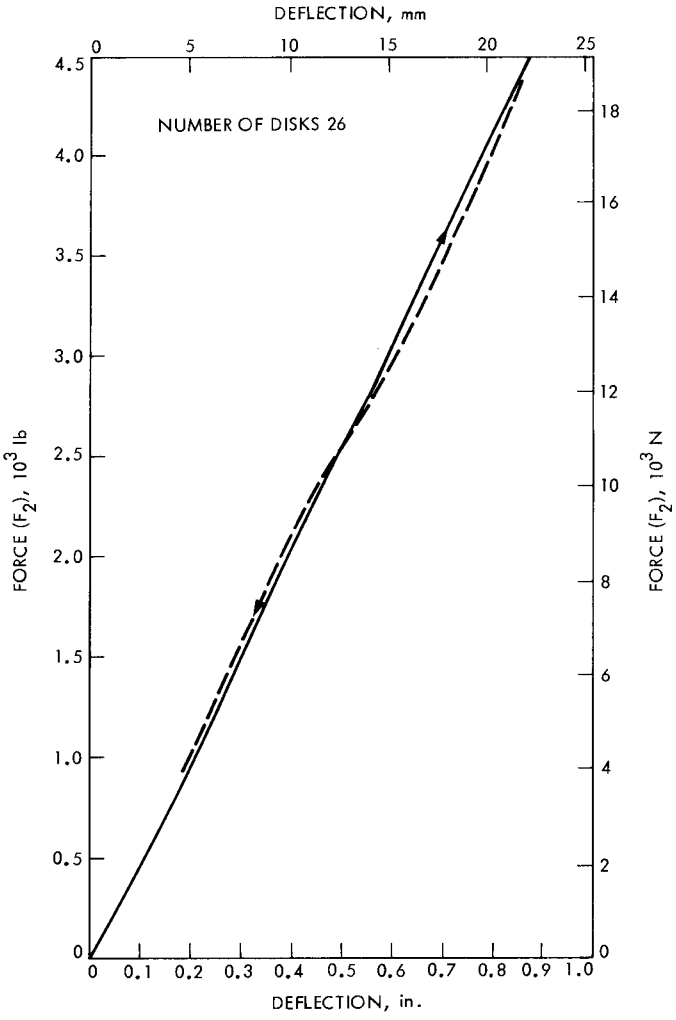

Fig. 21. Force versus deflection, measured, tension serial 4

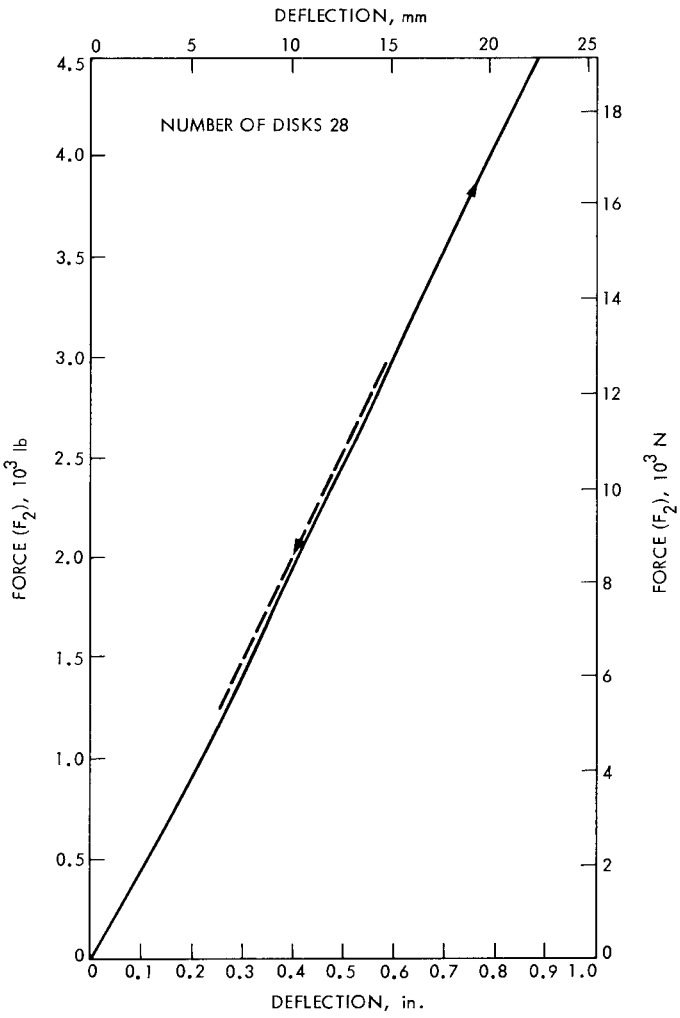

Fig. 22. Force versus deflection, measured, tension serial 5

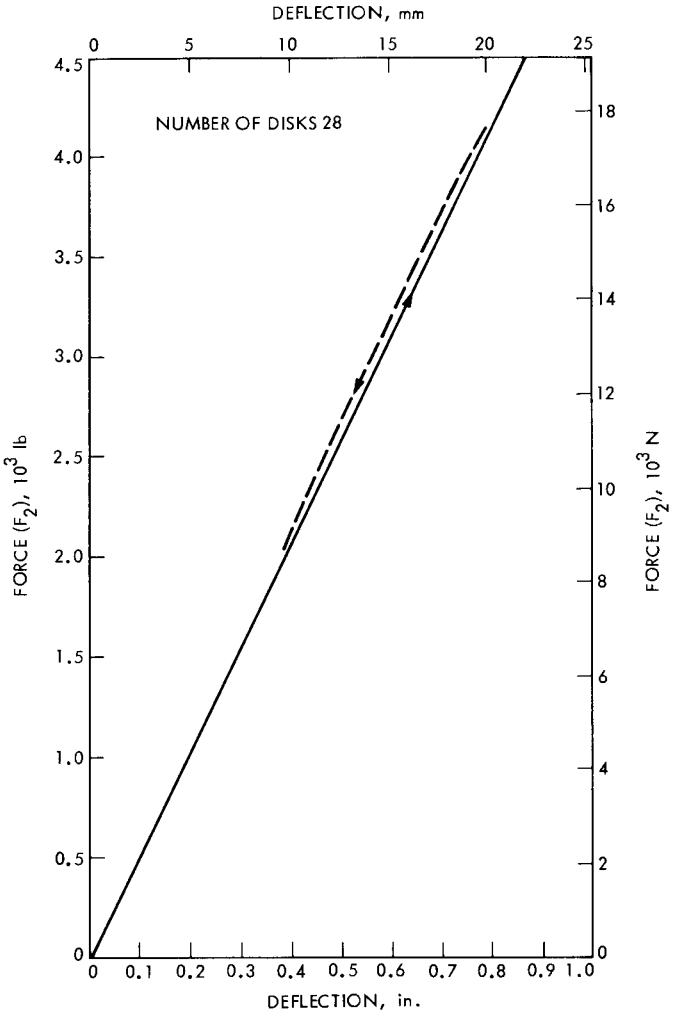

Fig. 23. Force versus deflection, measured, tension serial 6

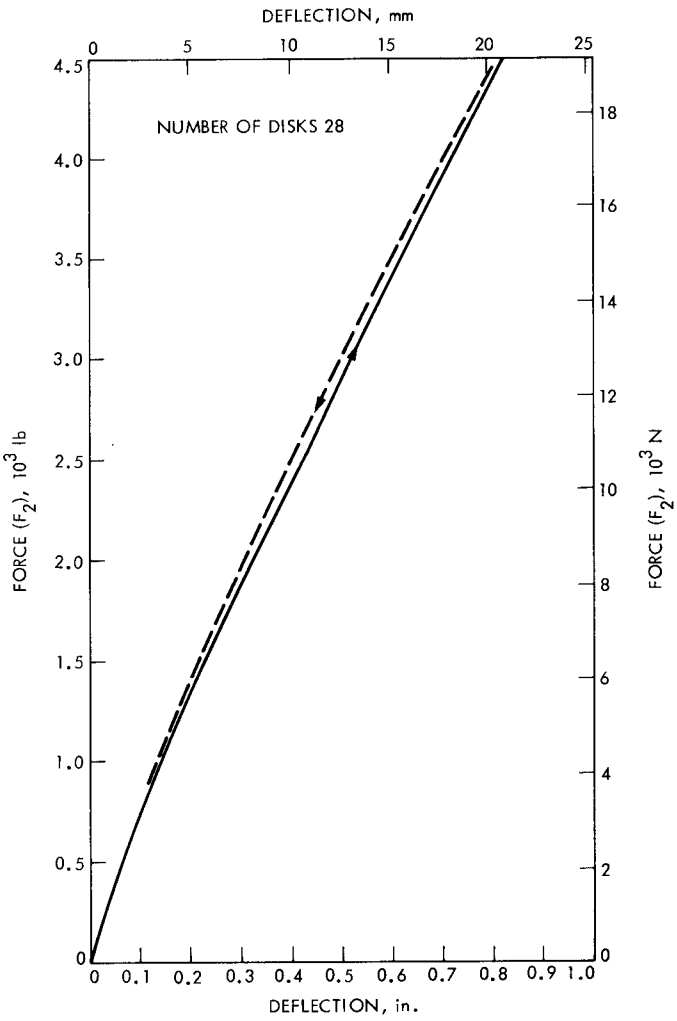

Fig. 24. Force versus deflection, measured, tension serial 7

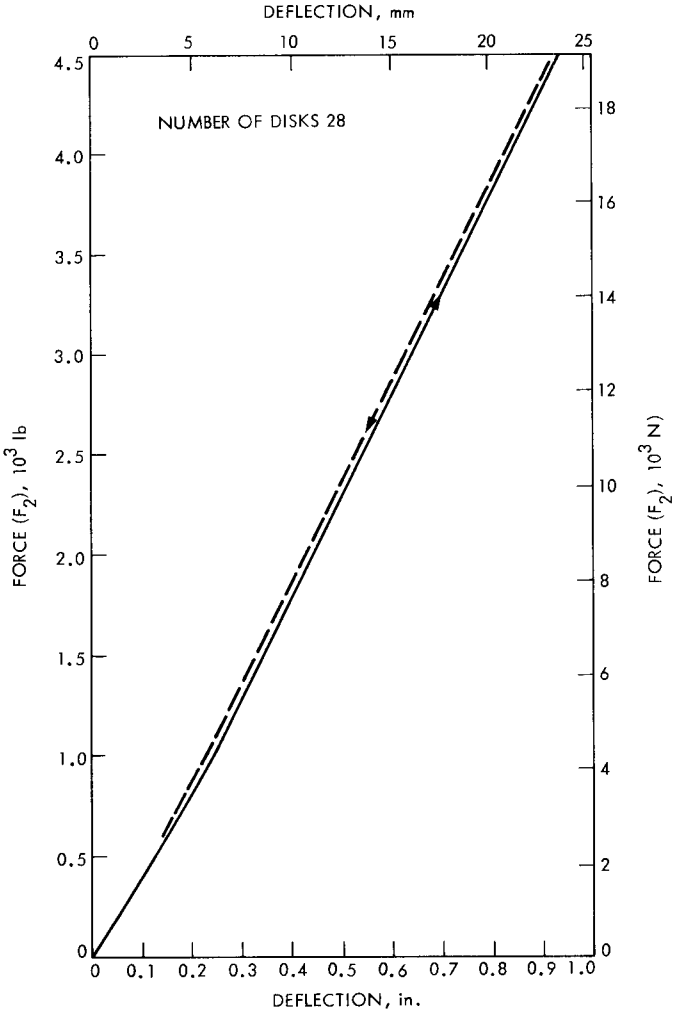

Fig. 25. Force versus deflection, measured, tension serial 8

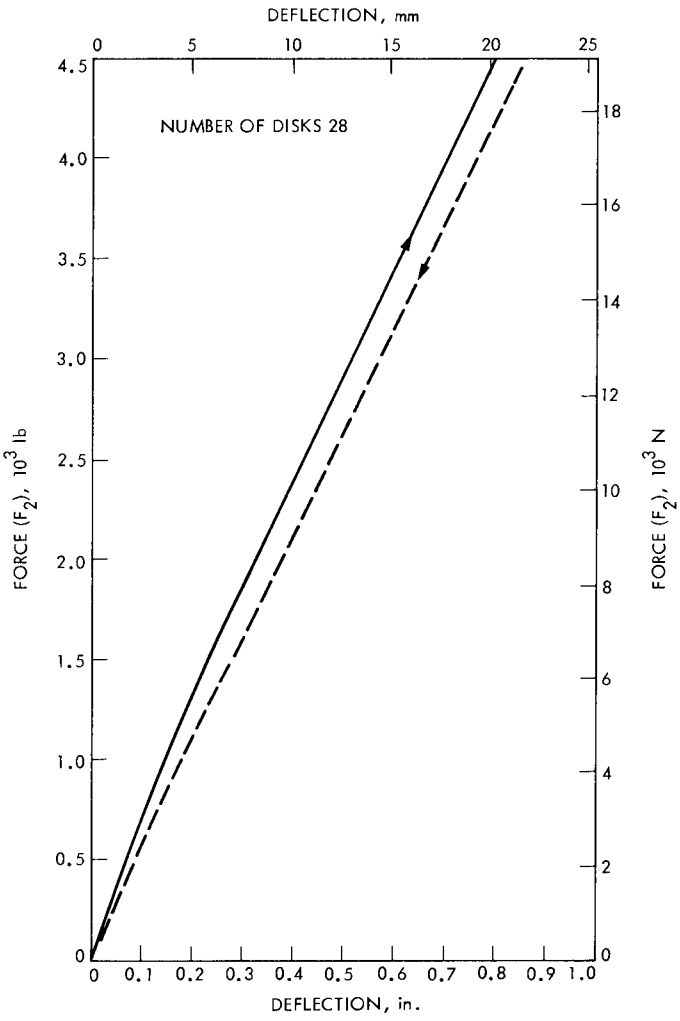

Fig. 26. Force versus deflection, measured, tension serial 9

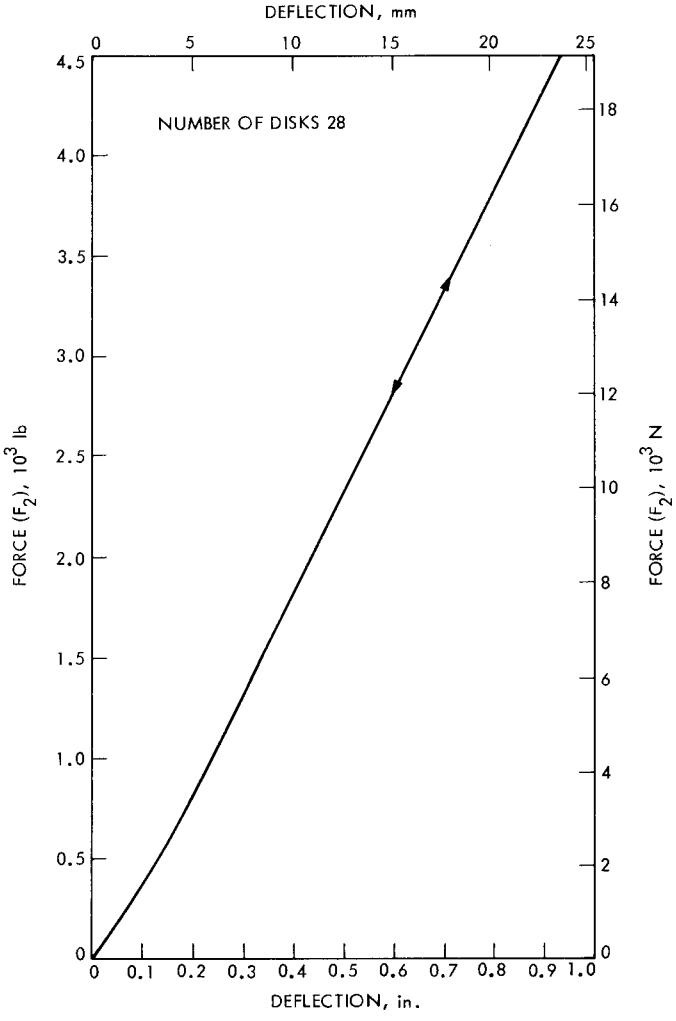

Fig. 27. Force versus deflection, measured, tension serial 10

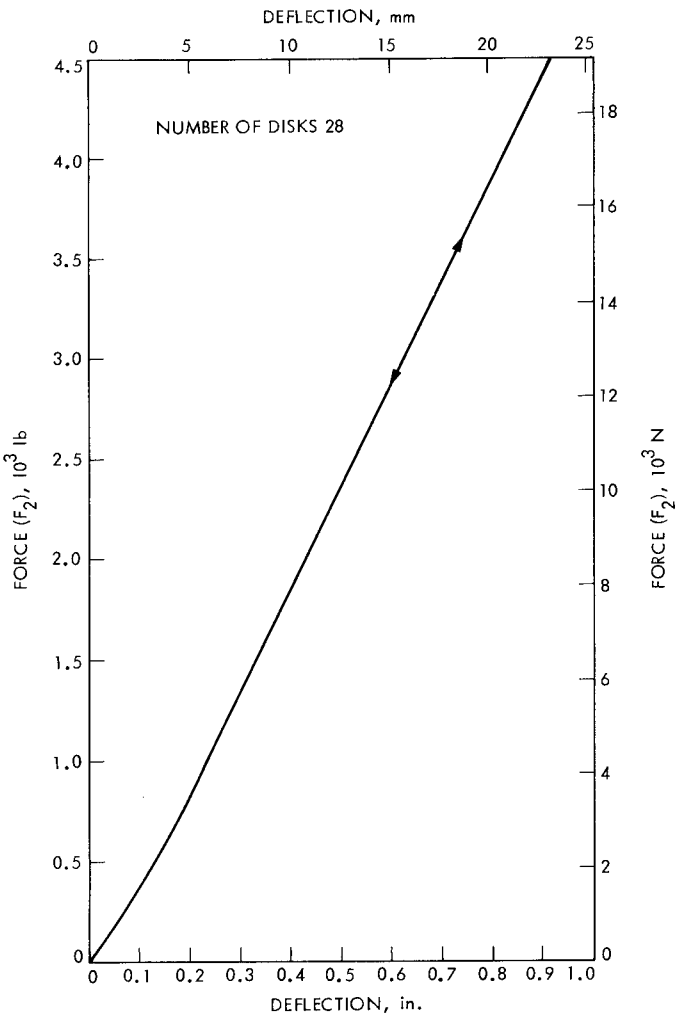

Fig. 28. Force versus deflection, measured, tension serial 11

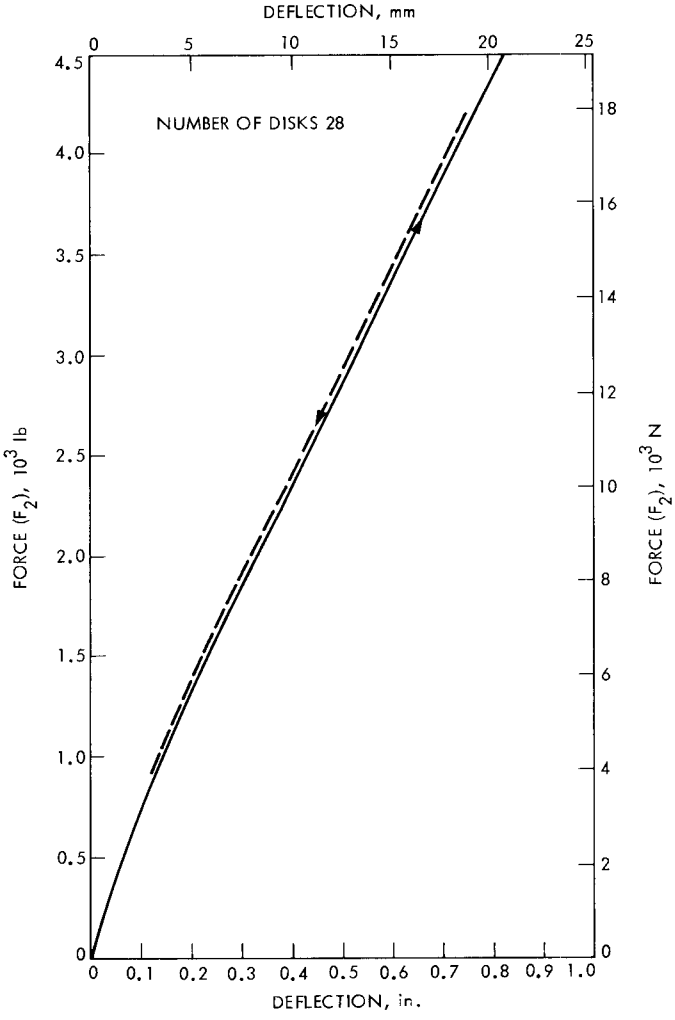

Fig. 29. Force versus deflection, measured, tension serial 12

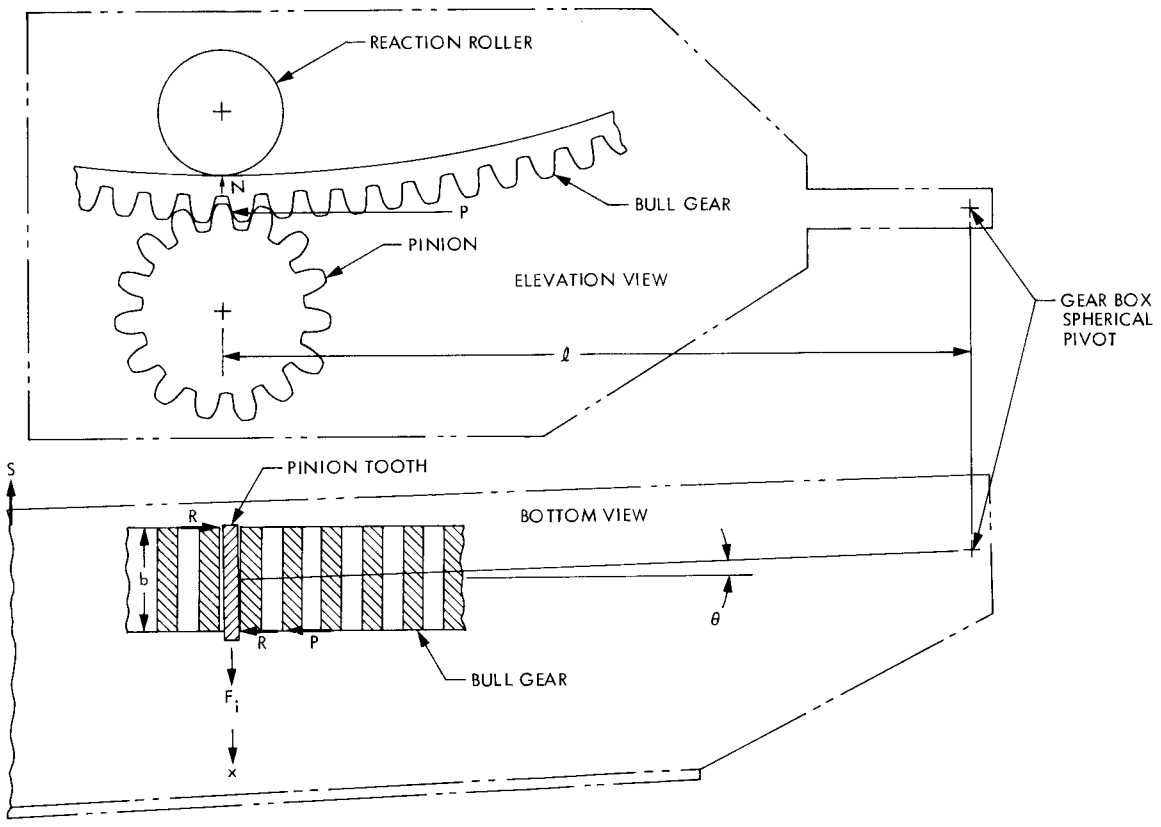

Fig. 30. Schematic of the elevation drive gears, showing forces considered

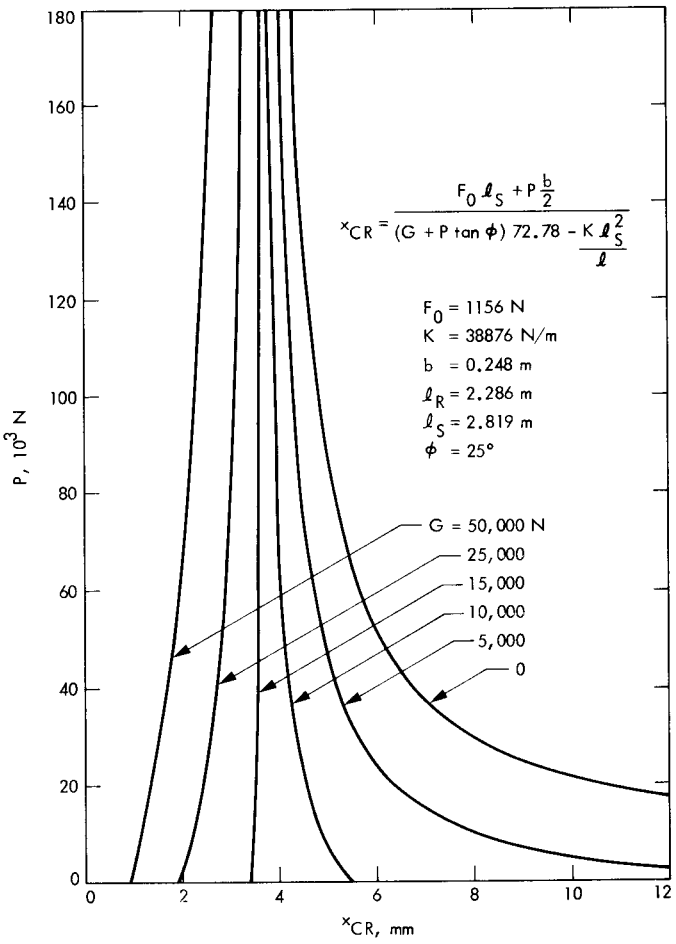

Fig. 31. Critical displacement, x_{CR}, versus tangential load P

Appendix A

Static Stability Criterion for Elevation Drive of the 64-Meter Antenna

In 1966, shortly after the completion of the 64-m antenna at DSS 14, the No. 1 elevation drive pinion ran off the bull gear. To prevent a recurrence, bronze shoes or rubbing blocks were added to the drive housing so as to bear against the edge of the bull gear whenever conditions promoted a tendency for the pinion to run off. The arrangement and support of the gear boxes, as shown in Figs. 1 and 2, is such as to allow the pinion to align itself perfectly with the teeth of the bull gear. There is a spherical joint at one end of the gear box and two vertical and one horizontal spring loaded struts near the other end. This provision for gear self-alignment also allows the possibility of instability. The tendency for instability comes from induced lateral forces acting on a misaligned roller, which for the case at hand is the back-up roller or gear separation reaction roller. The bull gear teeth are on the outside of a ring structure. The inside surface of the ring is smooth and accurately spaced radially from the gear tooth pitch cylinder. The reaction roller, which is attached to the gear box and is nominally parallel to the drive pinion, constrains the pinion to near perfect radial alignment with the bull gear teeth. Ideally the contact force on the reaction roller is equal to the gear separation force, but if there is a variation in the bull gear radius, the vertical spring loaded support struts are deflected, and the spring force is equilibrated by a change in the roller reaction.

The induced side force on a misaligned roller can be large as described in Ref. 1. If large enough, the roller side force can predominate over restoring forces with the result that instability occurs. The following analysis discusses the conditions which promote static instability. Such instability is possible only when the motion of the bull gear is from pinion to gear box pivot. The reverse motion cannot produce instability.

Figure 30 shows two views of a gear box. By summing moments about the pivot point, the stabilizing and unstabilizing effects can be compared. For the case where the misalignment is small enough so that both edges of the gear teeth are not grounded out against the mating gear, the R forces do not exist, and the instability inequality is:

$$F_i \ell_R > S \ell_s + P m \tag{1}$$

where P is the tangential force at the pitch line caused by pinion torque

$$S = F_0 + k x \frac{\ell_s}{\ell_R} \tag{2}$$

is the horizontal spring loaded strut force

F_0 is the initial preload spring force

k is the spring constant

x is lateral displacement of pinion or roller

ℓ_R is distance from pivot to roller or pinion

ℓ_s is distance from pivot to horizontal strut

m is distance from center of gear to force P

$F_i = NC$, the induced side force

N is the normal force on the roller

C is the side force coefficient

The normal force on the roller, N, is:

$$N = G + P \tan \phi \tag{3}$$

where G is the portion of N caused by gear box weight and ϕ is the pressure angle of the spur gear teeth. Substitute Eqs. (2) and (3) into (1) and obtain:

$$(G + P \tan \phi) C \ell_R > F_0 \ell_s + k \frac{\ell_s^2}{\ell_R} x + P m \tag{4}$$

It is desirable to express C as a function of x and this can be done by using the straight line portion of Fig. 3 of Ref. 1 which is a plot of C versus the misalignment angle of a cylindrical roller. The result is:

$$C = 72.78 \theta \tag{5}$$

where θ is the misalignment in radians. For the elevation drive,

$$\theta = \frac{x}{\ell_R} \tag{6}$$

Hence,

$$C = 72.78 \frac{x}{\ell_R} \tag{7}$$

Substitute Eq. (7) into Eq. (4) and obtain:

$$(G + P \tan \phi)\, 72.78\, x > F_0\, \ell_s + k\, \frac{\ell_s^2}{\ell_R}\, x + P m \qquad (8)$$

If the load on the misaligned pinion is triangularly distributed along the tooth width, b, m_1 is equal to $b/6$, whereas if the load is concentrated at the edge, $m_2 = b/2$. Both cases will be considered. The horizontal spring loaded strut (JPL Dwg. 9436181) has an F_0 value of 1156 N (260 lb) and a k value of 38876 N/m (222 lb/in.). A cursory check of the stiffness of the structure to which the horizontal strut attaches shows that practically all the flexibility is constituted by the spring loaded strut; therefore the small deflection of the structure will be ignored. When x is zero the left side of Eq. (8) is zero and the expressed inequality is not true; hence if Eq. (8) is converted to an equality, for finite values of x, and solved for x, the x value, called x_{CR}, represents the condition of neutral static stability. If an incidental displacement of the gear box should exceed x_{CR}, the displacement would increase, whereas an incidental displacement less than x_{CR} would be reduced.

$$x_{CR} = \frac{F_0\, \ell_s + P m}{(G + P \tan \phi)\, 72.78 - k\, \dfrac{\ell_s^2}{\ell_R}} \qquad (9)$$

Equation (9) is valid providing there is sufficient gear tooth backlash to allow one edge of tooth to be free. When instability occurs the lateral displacement, x, increases until both edges of the tooth are in contact and additional forces are developed. This will be discussed later.

It is desirable that x_{CR} be large from a static stability standpoint. From Eq. (9) it is clear that large F_0 promotes large x_{CR}. The quantity $(G + P \tan \phi)$ must not be negative or the roller would not be in contact with its track; hence large k also promotes large x_{CR}. Large m value also promotes large x_{CR}. If a small m value existed such that instability occurred, an increase in displacement would cause the small m value to shift to the larger m value; therefore it is proper to consider only the larger one, namely, $m_2 = b/2$. In other words the triangular distribution of tooth load will shift to corner loading as x increases. Equation (9) becomes

$$x_{CR} = \frac{F_0\, \ell_s + P\, \dfrac{b}{2}}{(G + P \tan \phi)\, 72.78 - k\, \dfrac{\ell_s^2}{\ell_R}} \qquad (10)$$

Equation (10) is plotted in Fig. 31 as x_{CR} versus P for various values of G for the particular values given in the figure which pertain to the elevation drive. The effect of G obviously is to reduce substantially the value of x_{CR}. Therefore it is extremely important that the vertical struts of the elevation drive be easily adjustable so that little dead weight portion of the gear box is resisted by the roller. If the bull gear has radial runout, as surely such a large gear will, then as the vertical struts change length, a finite G force will develop. Adjustments should be made to minimize the G force value.

The 64-m antenna elevation drives are counter-torqued against each other to give P values of approximately 66720 N at zero wind condition. At this P value x_{CR} is 5 mm for zero G and reduces to 3.7 mm for a G value of 10000 N. It is interesting to notice from Fig. 31 that a reduction in P increases the critical displacement, x_{CR}, for the smaller G values but decreases x_{CR} for the larger G values.

For the case of static instability, the lateral displacement, x, increases under the action of the forces considered above, until diagonal corners of the pinion are hard against adjacent teeth of the bull gear. At this time the corner forces R come into existence. Referring to Fig. 30 and summing moments about the gear box pivot, there is obtained the following balance of moments if equilibrium exists:

$$F_i\, \ell_R = S\, \ell_s + P\, \frac{b}{2} + R b \qquad (11)$$

The normal force, N, on the roller is now increased by the additional corner forces, R, and becomes:

$$N = G + P \tan \phi + 2R \tan \phi \qquad (12)$$

The induced force F_i is, as before,

$$F_i = NC = N\,(72.78)\, \frac{x}{\ell_R}$$

$$= 72.78\, \frac{x}{\ell_R}\, [G + P \tan \phi + 2R \tan \phi] \qquad (13)$$

Substitute Eqs. (2) and (13) into Eq. (11) and obtain:

$$(G + P \tan \phi + 2R \tan \phi)\, (72.78)\, x \geqslant F_0\, \ell_s + k\, \frac{\ell_s^2}{\ell_R}\, x + P\, \frac{b}{2} + R b \qquad (14)$$

Equation (14) is identical to Eq. (8) except for the addition of the terms containing R. Since instability is assumed to exist up to the time the R forces come about, Eq. (14) will be an inequality as indicated if the left side R term is greater than the right side R term, that is, if

$$2(72.78)\, x \tan \phi > b \tag{15}$$

the value of the lateral displacement x_3 at the time the R forces come about is a function of the gear backlash, ϵ, the gear width b, and the distance from pinion to pivot, ℓ_R. The value of this x_3 is:

$$x_3 = \frac{\ell_R \epsilon}{b} \tag{16}$$

The backlash range is 0.001020 to 0.000635 m, ℓ_R is 2.286 m, and b is 0.248 m, thus

$$x_3 = \frac{2.286}{0.248} \epsilon = 9.217\, \epsilon \tag{17}$$

which equals 0.0094 m to 0.00585 m. Substitute the smaller value of Eq. (17) into Eq. (15) and obtain:

$$2(72.78)\,(0.00585)\,(0.466) > 0.248 \tag{18}$$

$$0.396 > 0.248 \tag{19}$$

which shows that equilibrium does not exist for these conditions. The existence of R as a restoring moment causes the induced side force moment, $F_i \ell_R$, to increase by a greater amount than the restoring moment Rb. The result is that if an incidental lateral displacement exceeds x_{CR}, the displacement will continue and cause the pinion to run off the bull gear if pinion rotation continues, unless there are additional constraints such as the bronze rubbing shoe.

It is believed that this is the explanation for the pinion run-off that occurred in 1966 at DSS 14, and only a relatively small incidental lateral displacement was required because there was an excessive portion of the gear box dead weight being carried by the roller, that is, the G value of Fig. 31 was excessive.

Appendix B

Derivation of Strut Stiffness Ratios

The configurations of the elevation drives, lower and upper are shown respectively in Figs. 1 and 2. These figures show the locations of the spherical pivot, center of gravity, weight, vertical strut locations which are designated F_1 and F_2, β angles which represent direction displacements of strut upper ends as the drive unit rotates about the z axis, pinion position, and reaction roller. Schematic drawings of the spring loaded support struts are shown in Fig. 3.

Ideally the dead weight of the drive unit, or gear box, is supported by the spherical joint and the two vertical struts. The reaction roller, which rests against the inner surface of the bull gear ring, ideally reacts only the separating force between the pinion and bull gear, but if the bull gear has radial runout, as surely it will, the gear box is caused to rotate about its pivot, and this will change both the reaction roller load and the vertical strut loads. The primary objective of this analysis is to determine the proper ratio between the stiffnesses of the vertical struts so that when the gear box is forced to rotate slightly about the z axis, there will be no concomitant roll about the x axis. Such x axis roll would tend to misalign the pinion and roller. However, the stiffnesses of both vertical struts must be low enough to allow the gear box to align itself to the bull gear, if the bull gear should roll from its nominal position, without inducing large forces.

First the extension (or compression) ratio between the struts, such that gear box roll is avoided, must be calculated. This is done by referring to Fig. 4 which shows the lengths of extended and compressed struts in terms of the gear box rotation and other parameters identified in the figure.

Let δ be the bull gear radial runout. The gear box rotation α is:

$$\alpha = \frac{\delta}{\ell_R} \tag{1}$$

where ℓ_R is distance from pivot to roller. Substituting Eq. (1) into the expressions of Fig. 4 representing the lengths of the extended and compressed struts, it is easy to show that for small α values, extension and contraction both can closely be approximated by:

$$\Delta L = \frac{R}{\ell_R}\,\delta \cos\beta \tag{2}$$

For the expected bull gear runout of $\delta < 5$ mm, the vertical strut will tilt only a negligible amount; thus the effect on the horizontal moment arms of the struts may be ignored.

The ΔL's for the struts will be identified with the subscripts 1 and 2, for F_1 and F_2, and with subscripts L and U, for lower and upper gear boxes.

$$\Delta L_{1L} = \frac{123.5}{90}(\cos 10.35)\,\delta = 1.350\,\delta \tag{3}$$

$$\Delta L_{2L} = \frac{105}{90}(\cos 22.28)\,\delta = 1.080\,\delta \tag{4}$$

$$\Delta L_{1U} = \frac{128}{90}(\cos 30.15)\,\delta = 1.230\,\delta \tag{5}$$

$$\Delta L_{2U} = \frac{106}{90}(\cos 30.70)\,\delta = 1.013\,\delta \tag{6}$$

The required extension (or compression) ratios are:

$$\frac{\Delta L_{1L}}{\Delta L_{2L}} = \frac{1.350}{1.080} = 1.250 \tag{7}$$

for the lower gear box and

$$\frac{\Delta L_{1U}}{\Delta L_{2U}} = \frac{1.230}{1.013} = 1.214 \tag{8}$$

for the upper gear box, which are the required extension ratios for no roll of the gear boxes.

For the condition of perfect roller alignment, the roller force F_R produces no moment about the x axis. If the gear box is rotated about the z axis without rolling about the x axis, as is desired, the moment equilibrium equation about the x axis is:

$$a_1\,\Delta F_1 = a_2\,\Delta F_2 \tag{9}$$

where the moment arms a_1 and a_2 are identified in Figs. 1 and 2 and ΔF_1 and ΔF_2 are force increments in vertical struts No. 1 and No. 2 respectively, and are:

$$\Delta F_1 = K_1\,\Delta L_1 \tag{10}$$

$$\Delta F_2 = K_2 \Delta L_2 \tag{11}$$

Divide Eq. (11) by (10) and obtain:

$$\frac{K_2}{K_1} = \frac{\Delta F_2}{\Delta F_1}\frac{\Delta L_1}{\Delta L_2} \tag{12}$$

Substitute $\Delta F_2/\Delta F_1$ from Eq. (9) into (12) and obtain:

$$\frac{K_2}{K_1} = \frac{a_1}{a_2}\frac{\Delta L_1}{\Delta L_2} \tag{13}$$

as the desired ratio between the stiffnesses of the two vertical struts.

Now the strut forces F_1 and F_2 will be calculated. Again assume that the roller reaction, F_R, is uniformly distributed so that it does not produce a moment about the x axis. Sum moments about axes x and z and obtain:

$$a_1 F_1 + a_2 F_2 = a_w W \tag{14}$$

where W is gear box weight

$$\ell_1 F_1 - \ell_2 F_2 = \ell_w W - \ell_R F_R \tag{15}$$

From Eq. (14)

$$F_2 = \frac{a_w}{a_2} W - \frac{a_1}{a_2} F_1 \tag{16}$$

A plot of Eq. (16) is in Fig. 5. Substitute Eq. (16) into (15) and obtain:

$$\ell_1 F_1 - \ell_2 \left[\frac{a_w}{a_2} W - \frac{a_1}{a_2} F_1\right] = \ell_w W - \ell_R F_R \tag{17}$$

Solve Eq. (17) for F_1 and obtain:

$$F_1 = \left[\frac{\ell_w + \ell_2 \dfrac{a_w}{a_2}}{\ell_1 + \ell_2 \dfrac{a_1}{a_2}}\right] W - \left[\frac{\ell_R}{\ell_1 + \ell_2 \dfrac{a_1}{a_2}}\right] F_R \tag{18}$$

From Eq. (14)

$$F_1 = \frac{a_w W}{a_1} - \frac{a_2}{a_1} F_2 \tag{19}$$

Substitute Eq. (19) into Eq. (15) and obtain:

$$F_2 = \left[\frac{\ell_1 \dfrac{a_w}{a_1} - \ell_w}{\ell_2 + \ell_1 \dfrac{a_2}{a_1}}\right] W + \left[\frac{\ell_R}{\ell_2 + \ell_1 \dfrac{a_2}{a_1}}\right] F_R \tag{20}$$

Various values of F_R have been calculated from Eq. (20) and are shown in Fig. 5.

From Eqs. (18) and (20) it can be seen that as F_R becomes finitely positive, F_1 reduces and F_2 increases. From Figs. 1 and 2 it is clear that as the gear boxes rotate clockwise about the z axis, both F_1 and F_2 struts must extend. Since F_1 is a compression strut its extension represents a reduction in load; F_2 is a tension strut and so its extension represents an increase in load. If the gear box has been perfectly aligned so that the reaction roller uniformly clears the bull gear by an infinitesimal amount, F_R is zero and F_1 and F_2 can be calculated from Eqs. (18) and (20). From this condition let the bull gear run out radially by the amount δ. The quantities ΔF_1 and ΔF_2 can be calculated using Eqs. (3), (4), (5), and (6) together with Eqs. (10) and (11) obtaining:

$$\Delta F_{1L} = K_{1L}\, 1.350\, \delta \tag{21}$$

$$\Delta F_{2L} = K_{2L}\, 1.080\, \delta \tag{22}$$

$$\Delta F_{1U} = K_{1U}\, 1.230\, \delta \tag{23}$$

$$\Delta F_{2U} = K_{2U}\, 1.013\, \delta \tag{24}$$

The roller reaction force, F_R, may be calculated by substituting these values of ΔF for F_1 and F_2 of Eqs. (18) and (20) respectively, with W set to zero since incremental loading due to runout is now being considered. There are obtained:

$$F_{RL} = 2.2005\, K_{2L}\, \delta \tag{25}$$

$$F_{RU} = 1.9048\, K_{2U}\, \delta \tag{26}$$

Since the dimensionless coefficients of Eqs. (25) and (26) vary only about 7% from their mean value, it is feasible to select a common value for K_{2L} and K_{2U}. The important feature is that the ratio between K_2 and K_1 be in accordance with Eq. (13) which when evaluated becomes:

$$\left(\frac{K_2}{K_1}\right)_L = 1.770 \tag{27}$$

$$\left(\frac{K_2}{K_1}\right)_U = 1.709 \tag{28}$$

where the subscripts L and U designate lower and upper gear boxes respectively.

These stiffness ratios are the ideal ones which would both prevent gear box roll about the x axis and insure uniform loading along the reaction roller length. From practical considerations it is impossible to obtain these stiffness ratios exactly. The following analysis will show over what range the stiffness ratio can vary without allowing x axis roll but by allowing nonuniform loading along the roller length. The roller loading now being considered is caused by bull gear radial runout only. (The primary load on the roller is caused by the gear separation force and this will be discussed later.)

Consider that the roller force, F_R, is a concentrated force applied to the gear box at the roller position but displaced the distance h (see Fig. 2) along the roller axis from the mid-point of the roller length. The three supports of the gear box are the spherical pivot and the F_1 and F_2 struts which have reactions ΔF_1 and ΔF_2 respectively. Sum moments about the x axis and obtain:

$$\Delta F_1 a_1 - \Delta F_2 a_2 = \frac{F_R h}{\cos\theta} \tag{29}$$

Sum moments about the z axis and obtain:

$$\Delta F_1 \ell_1 + \Delta F_2 \ell_2 = F_R \ell_R \tag{30}$$

Substitute Eq. (30) into (29) and obtain:

$$h = \frac{(\Delta F_1 a_1 - \Delta F_2 a_2)\ell_R \cos\theta}{(\Delta F_1 \ell_1 + \Delta F_2 \ell_2)} \tag{31}$$

Using Eqs. (10) and (11) together with Eqs. (3), (4), (5), and (6), and letting $\lambda = K_1/K_2$, h is evaluated for the lower and upper gear boxes as:

$$\frac{h_L}{\ell_R} = \frac{(1.350 a_1 \lambda - 1.080 a_2)\cos 7.683^\circ}{(1.350 \ell_1 \lambda + 1.080 \ell_2)}$$

$$= \frac{26.423\lambda - 14.931}{163.957\lambda + 105.397} \tag{32}$$

$$\frac{h_U}{\ell_R} = \frac{(1.230 a_1 \lambda - 1.013 a_2)\cos 45.25^\circ}{(1.230 \ell_1 \lambda + 1.013 \ell_2)}$$

$$= \frac{17.102\lambda - 10.006}{135.521\lambda + 92.142} \tag{33}$$

From Eqs. (32) and (33) the corresponding values of λ and h_L/ℓ_R shown in Table 1 are obtained. The length of the cylindrical part of the roller is 71.43 mm and ℓ_R is 2286 mm. Thus if the concentrated force F_R were located 71.43/2 mm from the roller center, h/ℓ_R would be 0.01562. The maximum value of h for which stability prevails is 35.71 mm, since if h exceeded this, the concentrated force would be beyond the cylindrical part of the roller and tilting would occur. Therefore if the stiffness ratio of the lower struts, K_1/K_2, lies between 0.460 and 0.694, tilting would not occur. If the stiffness ratio of the upper struts, K_1/K_2, lies between 0.446 and 0.760, tilting will not occur. The stiffnesses of the actual compression struts are given by the slopes of the force versus deflection curves shown in Figs. 6 through 17. The stiffnesses of the actual tension struts are given by the slopes of the force versus deflection curves shown in Figs. 18 through 29. These curves do not necessarily have constant slopes; therefore it is necessary to know the approximate values of F_1 and F_2 and these can be taken from Fig. 5 for the appropriate values of the reaction roller force F_R. The F_R values can be calculated from Eqs. (25) and (26) if the bull gear radial runout, δ, is known. From measurements made at DSS 14 in March 1980, at DSS 43 in 1980, and at DSS 63 in June 1980, the total excursions of the bull gear radial runouts were respectively 5.1 and 4.3 mm at DSS 14, 2.79 and 5.80 mm at DSS 43, and 1.14 and 1.65 mm at DSS 63. Using half the largest of these together with the K_2 value from Fig. 28, namely 18000/0.02005 Newtons per meter, Eqs. (25) and (26) yield

$$F_{RL} = \frac{2.2}{2}\frac{18000}{0.02005}0.0058 = 5728\ \text{N}$$

or 1288 lb and

$$F_{RU} = \frac{1.9}{2}\frac{18000}{0.02005}0.0058 = 4947\ \text{N}$$

or 1112 lb as approximations for the maximum F_R value caused by bull gear runout only. Taking the means between these estimated maximum F_R values and zero F_R values, there are obtained 644 lb and 556 lb respectively for the lower and upper gear boxes. For these mean values the F_1 and F_2 coordinates from Fig. 5 are:

$$F_{1L} = 13450\ \text{lb}$$

F_{2L} = 1400 lb

F_{1U} = 13280 lb

F_{2U} = 2400 lb.

It is for the foregoing F values that the strut spring constants will be compared to determine if the gear boxes will be free of rolling displacement as the bull gear undergoes radial run-out. These stiffness ratios are set out in Table 2 from which it may be seen that all ratios are within the desired range.

Appendix C

Outline for Removing, Installing, and Adjusting the Vertical Struts

The new vertical compression strut (JPL Dwg. 9477047) and the new vertical tension strut (JPL Dwg. 9477064) were installed and aligned essentially as per the following outline.

(1) Bull gear radial runout measurements made at DSS-63 were approximately one millimeter total excursion. For such small runouts the vertical struts may be installed and adjusted at any elevation angle. At DSS 43 the radial runout is 3 mm for one bull gear and 6 mm for the other. The mean compression or extension of the struts should be determined by measuring dimensions a and A of Fig. 3 for each gear box, over the elevation angle range. The adjustment of the new struts should be made at the elevation angle corresponding to the mean lengths. At DSS 14 the bull gear radial runouts are 4.3 mm and 5.1 mm. The proper DSS 14 elevation angles for adjusting the vertical struts are 65°, 60°, 71°, and 71° for gear boxes numbers 1, 2, 3, and 4 respectively.

(2) To remove a compression strut, the compressive load must be locked in by screwing in four 25.4-mm-diameter bolts until their ends contact the spring piston, thus preventing sudden expansion of the strut upon release of the gear box weight loading. The gear box must safely be supported by auxiliary jacks or hoists. Then the strut attachments may be removed. The new compression struts were compressed to 60000 N (13500 lb) and the corresponding A dimensions are shown in Figs. 6 through 17. Four 25.4-mm-diameter bolts locked in this compressive force, and in this condition the new compressive struts were installed by adjusting the large bronze nut as required. The tension strut was installed by adjusting its bronze nut as required.

(3) The auxiliary supports were removed allowing the gear box weight to be transferred to the new vertical struts and the reaction roller.

(4) To insure that there was no load on the drive pinion, the gear box input shaft was set near the middle of its backlash range. The four 25.4-mm-diameter bolts which locked in the compressive load were retracted. Then the bronze nuts of the compressive and tension struts were adjusted until a clearance was obtained between the reaction roller and bull gear back side. This was determined by using a thickness gage to verify clearance.

(5) The reaction roller was removed and the bronze nuts of the compression and tension struts further adjusted so that when the reaction roller was reinstalled, its clearance with the back side of the bull gear would be uniform. This was done by making measurements between the bull gear and the roller shaft housings.

(6) The dimensions a and A for the tension and compression struts respectively were measured. Dimension a for the unloaded tension strut had been previously recorded. A comparison of dimensions A and a with the force deflection curves shown respectively in Figs. 6 through 17 and Figs. 18 through 29, allow the forces in the struts to be determined for the condition of no load on the reaction roller.

(7) The reaction roller was reinstalled and the adjusting bronze nuts of the tension and compressive struts were safetied.

(8) The final adjustments of the gear boxes were made by adjusting the horizontal strut so as to optimize the pinion to bull gear teeth alignment. Further adjustments to the vertical struts would be necessary only if their springs should change their stiffnesses or if additional weight were added to the gear boxes. Such can be determined by setting the elevation angle at the proper position as given in step 1 and with the servo drive turned off, determining whether a clearance exists between the reaction roller and the bull gear back side.

(9) After the final adjustment, the change in lengths of the compression and tension struts, dimensions A and a, as a function of elevation angle, were measured and recorded.

The initial alignment dimensions for the new vertical struts at DSS-14 are shown in Table 3.